Applied Physics Letters

Electronically steerable ultrasound-driven long narrow air stream

Cite as: Appl. Phys. Lett. **111**, 064104 (2017); https://doi.org/10.1063/1.4985159
Submitted: 26 May 2017 • Accepted: 29 July 2017 • Published Online: 11 August 2017

Keisuke Hasegawa, Liwei Qiu, Akihito Noda, et al.

COLLECTIONS

Paper published as part of the special topic on Acoustic Tweezers

EP This paper was selected as an Editor's Pick

APPLIED PHYSICS LETTERS 111, 064104 (2017)

Electronically steerable ultrasound-driven long narrow air stream

Keisuke Hasegawa,[1] Liwei Qiu,[2] Akihito Noda,[3] Seki Inoue,[4] and Hiroyuki Shinoda[1,4]
[1]Graduate School of Frontier Sciences, The University of Tokyo, 5-1-5 Kashiwanoha, Kashiwa-shi, Chiba-ken 277-8561, Japan
[2]Center for Advanced Intelligence Project, RIKEN, 1-4-1 Nihonbashi, Chuo-ku, Tokyo 103-0027, Japan
[3]Department of Mechatronics, Nanzan University, 18 Yamazato-cho, Showa-ku, Nagoya 466-8673, Japan
[4]Graduate School of Information Science and Technology, The University of Tokyo, 7-3-1 Hongo, Bunkyo-ku, Tokyo 113-0033, Japan

(Received 26 May 2017; accepted 29 July 2017; published online 11 August 2017)

Acoustic streaming, which is the unidirectional movement of a medium driven by its internal intense acoustic vibrations, has been known for more than a century. Despite the long history of research, there have been no scientific reports on the creation of long stretching steerable airflows in an open space, generated by ultrasound. Here, we demonstrated the creation of a narrow, straight flow in air to a distance of 400 mm from an ultrasound phased array emitting a Bessel beam. We also demonstrated that the direction of the flow could be controlled by appropriately tuning the wavefronts of the emission from the phased array. Unlike conventional airflows such as those generated by jets or fans, which decelerate and spread out as they travel farther, the flow that we created proceeded while being accelerated by the kinetic energy supplied from the ultrasound beam and keeping the diameter as small as the wavelength. A flow of 3 m/s with a 10 mm diameter extended for several hundreds of millimeters in a room that was large enough to be regarded as an open-boundary environment. These properties of the generated flow will enable fine and rapid control of three-dimensional airflow distributions. [http://dx.doi.org/10.1063/1.4985159]

Sound yields flows—this fact has been known among researchers for more than one hundred years,[1,2] and many sophisticated theoretical studies have been conducted.[3–6] On the other hand, actual generation of sound-driven flows is limited to specific situations such as a liquid confined in a container.[7–9] This phenomenon, called acoustic streaming, is classified into several types based on their length in relation to the wavelength.[10] Among them, reported examples of straight flows that stretch longer than the wavelength are small in number, including recent underwater work that succeeded in generating a narrow, long flow[11,12] and a report on the qualitative observation of such an airflow.[13] This is presumably because a straight-shaped density profile of sound energy with sufficient intensity is required for generating such flows, which are not easily accomplished with ordinary sound sources. Nevertheless, if it were possible to create strong, localized flows out of sound irradiation, this would be applicable to new kinds of industrial and academic methodologies.

Here, we describe a method of generating a steerable, narrow, straight airflow located away from a phased array of ultrasound transducers which forms an acoustic Bessel beam. The generated ultrasound-driven flow is accelerated while proceeding due to the kinetic energy supplied from the ultrasound field, which is different from conventional jet-driven flows that merely attenuate and dissipate as the farther they travel. The highest-velocity spot can be located away from the sound source, as if virtual floating jets or fans were arranged along the flow in air. This mid-air blowing property of the flow would be greatly advantageous in the context of flexible arrangements of devices in practical applications. The generated flows were strong enough to be easily felt by the hand and to strongly guide water vapor in a desired direction. Note that all of these phenomena were verified in air of normal pressure and temperature, not in extreme environments.

When the sound sources are sinusoidal, the driving force per unit volume $\boldsymbol{F}$ of the resulting acoustic streaming is proportional to the acoustic intensity $\boldsymbol{I}$, which is equivalent to the temporally averaged acoustic power:[14]

$$\boldsymbol{F} = 2\frac{\alpha}{\rho c}\boldsymbol{I}, \tag{1}$$

where ρ is the density of the medium, c is the sound velocity in the medium, and α is the sound absorption coefficient. Note that $\boldsymbol{F}$ and $\boldsymbol{I}$ are both vectors that are oriented in the direction of sound propagation. From this relation, it is expected that a narrow, straight flow can be obtained from an ultrasound beam that also has a narrow, stretching acoustic energy intensity.

A Bessel beam would be a suitable example of such an acoustic beam. Bessel beams were originally discussed in optical disciplines[15] and are known for their non-diffracting propagation. A Bessel beam contains most of its energy centralized around the propagation axis over a considerably long distance. The cross-section of the beam has a concentric energy distribution that is technically described as a solution of Bessel's differential equation. The cross-sectional diameter can be as small as the wavelength. Therefore, if one wants a narrower beam, a sound source with a higher frequency is required. The generation of Bessel beams has been realized in many studies both in optical[16–19] and acoustic disciplines.[20–23] The common basic idea to generate the beam is to prepare a conic sound source so that the irradiated wavefronts will be symmetric around the propagating axis, and consequently, the sound energy will concentrate around the axis. Although a specially designed massive sound source could be used to this end, we instead used an ultrasound phased array, which is an integrated set of ultrasound transducers whose individual output phase shifts are electronically tunable. With proper setting of the phase-delayed emissions from multiple sources, the wavefront of the generated ultrasound can be controlled. For generating a Bessel beam, the phase shift at each transducer should be proportional to the distance between the transducer itself and a virtual conical sound source whose apex is on the irradiation plane of the array (Fig. 1). Thus, a phased array is advantageous in generating sound fields that are flexibly controlled by an identical device.[24]

Note that the following discussion about phase engineering is based on a linear acoustics framework. The nonlinear manner of the acoustic streaming is not taken into consideration. Nevertheless, the nonlinear phenomenon only happens where the sound intensity is sufficiently high, and the high-energy region is determined by the linear phase engineering technique described below.

Based on Huygens' principle, multiple point wave sources that create a conical wavefront can be considered as a virtual acoustic cone-shaped source resulting in an acoustic Bessel beam that propagates along the central axis of the cone. Each source located at $\boldsymbol{r} = [x\,y\,z]^T$ should have a phase shift that is proportional to the distance from the virtual source cone (here, ^{T} means the transpose of a vector). Suppose that the z axis is parallel to the axis of the cone and that θ_z is the angle between the side of the cone and the xy-plane. Geometrically, the distance between the cone and the source, d, is given by

$$d = \sin\theta_z\sqrt{x^2+y^2} - \cos\theta_z z. \tag{2}$$

Note that the value of d here is "signed." It takes a negative value when $\boldsymbol{r}$ is "inside" the cone, corresponding to giving negative phase shifts where the wavefront of the cone arises behind the ultrasound sources. With the array aperture A (the diameter for a circular array), the central depth of the beam, z_c, is given by

$$z_c = \frac{A}{4\tan\theta_z}. \tag{3}$$

This is roughly where the acoustic intensity takes its maximum value. Decreasing θ_z to zero means that the beam reaches farther. At the same time, the generated wavefront as a whole becomes more similar to a plane wave, resulting in a less-concentrated beam around the z-axis. Thus, there is a tradeoff between the beam concentration and its reaching distance.

The case of a tilted Bessel beam is now discussed. Let $\boldsymbol{n} = [n_x\,n_y\,n_z]^T$ be a unit vector that indicates the direction of propagation in which $n_x^2+n_y^2+n_z^2 = 1$ holds. By tilting the cone axis $\boldsymbol{e}_z = [0\,0\,1]^T$ toward $\boldsymbol{n}$, a Bessel beam oriented along $\boldsymbol{n}$ can be obtained. The corresponding rotational operation can be expressed by a rotation axis $\boldsymbol{v}$ with its angle $\theta_{\boldsymbol{v}}$. These are given by

$$\boldsymbol{v} = \frac{\boldsymbol{e}_z \times \boldsymbol{n}}{|\boldsymbol{e}_z \times \boldsymbol{n}|}, \tag{4}$$

$$\theta_{\boldsymbol{v}} = \sin^{-1}(|\boldsymbol{e}_z \times \boldsymbol{n}|). \tag{5}$$

In order to realize the tilted cone source, the distance calculation should be done with transducer positions that are rotated in line with the rotational operation described above. According to Rodrigues' rotational rule, the rotated transducer position $\boldsymbol{R} = [X\,Y\,Z]^T$ about a rotational axis $\boldsymbol{v}$ with a rotational angle $-\theta_{\boldsymbol{v}}$ is given by

$$\boldsymbol{R} = \cos\theta_{\boldsymbol{v}}\boldsymbol{r} - \sin\theta_{\boldsymbol{v}}(\boldsymbol{v}\times\boldsymbol{r}) + (1-\cos\theta_{\boldsymbol{v}})(\boldsymbol{v}^T\boldsymbol{r})\boldsymbol{v}. \tag{6}$$

Therefore, the proper phase delay ϕ that is imposed on the transducer is

$$\phi = k(\sin\theta_z\sqrt{X^2+Y^2} - \cos\theta_z Z), \tag{7}$$

where k is the wavenumber of the ultrasound.

Figure 1 shows a schematic explanation of the wavefronts generated with an array of sound sources.

By substituting $x - x_0$ and $y - y_0$ for x and y, respectively, one obtains a propagation axis rooted at (x_0, y_0). Although this might be evident, it is important to state that the beam does not have to be fixed at the center of the array from an application perspective.

We measured the spatial distribution of an actual airflow that arose from an ultrasound Bessel beam that we generated.

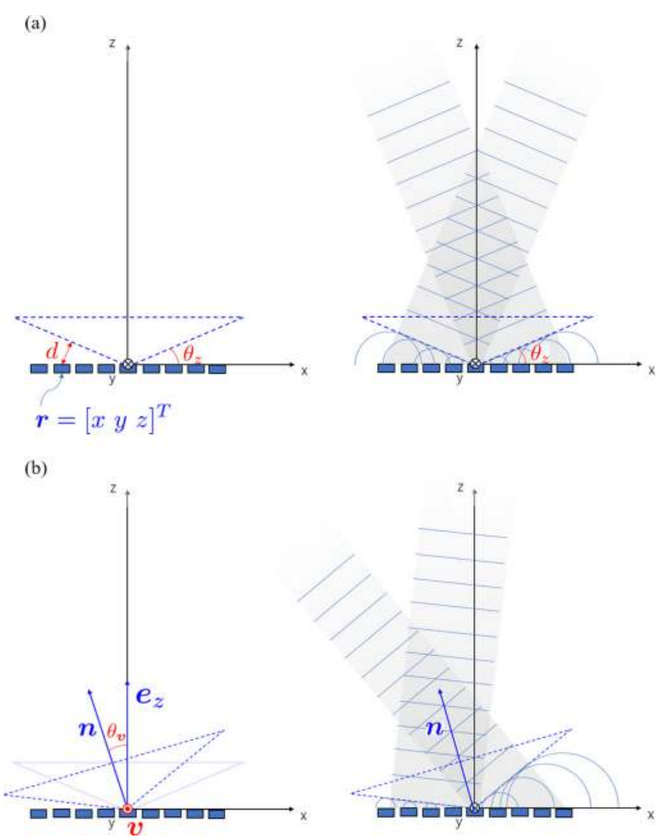

FIG. 1. Virtual cone-shaped sound source and collective wavefront emitted from arrayed multiple point sources when the resulting Bessel beam is (a) perpendicular to the array and (b) tilted.

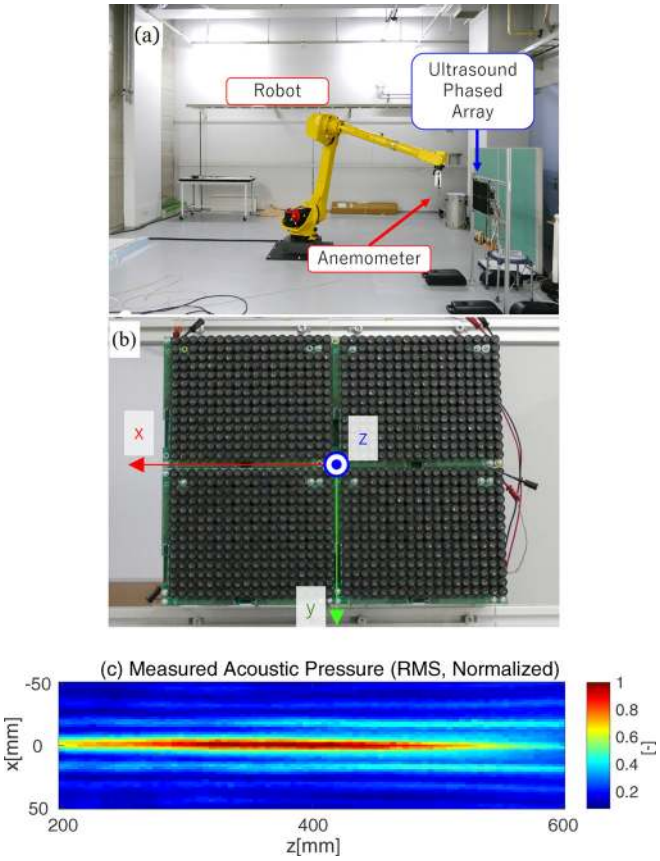

FIG. 2. (a) Measurement setup. (b) Ultrasound transducer array composed of four device units. The defined coordinates in the experiment are also depicted. (c) Measurement of RMS pressure with an upright Bessel beam that is identical to the one whose wind velocity distribution is measured and shown in Fig. 3. Its maximum sound level was 167 dB (where the normalized value is 1).

Figures 2(a) and 2(b) show the experimental setup. We used an ultrasound phased array composed of four units [Fig. 2(b)] for generating the ultrasound Bessel beam. Each unit contained 249 ultrasound transducers. The array was placed away from the wall of the room in order to alleviate the effect of air circulation and to avoid generating standing waves. The resonant frequency of the transducers was 40 kHz. The maximum power consumption of each unit was approximately 50 W. The aperture constructed by the units was a rectangle of size 373.8 mm (x-axis) × 292.7 mm (y-axis). During all of the following measurements, we generated Bessel beams with the value of θ_z set to 18°.

To measure the airflow velocity, we used a hot-wire anemometer (KANOMAX CLIMOMASTER 6501-C0) attached to a robot hand (FANUC M710-iC 20L) scanning in two-dimensional planes. The probe of the anemometer was KANOMAX 6533-21 topped with a spherical sensing tip whose diameter was 2.5 mm that had no directivity around azimuthal angles. It should be clearly noted that in the measurement, we only captured the absolute value of flow velocity, that is, not including its direction. In preliminary measurements, turbulence was observed, and therefore, we set the sensor output to be a temporal moving average of the measurements during the most recent 10 s period, which was converted into a DC voltage. Note that this fluctuation was not avoidable even by averaging the output of the anemometer for one minute.

We performed the scanning with three sets of measurement regions in order to evaluate the degree of the spatial concentration in stream velocity for a non-tilted beam. These three sets are given as follows: (a) the xz-plane where $-200\,\text{mm} \leq x \leq 200\,\text{mm}$ (every 20 mm) and $100\,\text{mm} \leq z \leq 1500\,\text{mm}$ (every 100 mm), (b) the xz-plane where $-50\,\text{mm} \leq x \leq 50\,\text{mm}$ (every 5 mm) and $200\,\text{mm} \leq z \leq 600\,\text{mm}$ (every 20 mm), and (c) a plane where $-20\,\text{mm} \leq x \leq 20\,\text{mm}$ (every 2 mm) and $-20\,\text{mm} \leq y \leq 20\,\text{mm}$ (every 2 mm), and $z = 400\,\text{mm}$. We also generated a tilted Bessel beam with $\theta_{\boldsymbol{v}} = 20°$ and $\boldsymbol{v} = [0\ -1\ 0]^T$, where the resulting wind velocity was scanned within the xz-plane where $200\,\text{mm} \leq z \leq 600\,\text{mm}$ (every 20 mm) and $-200\,\text{mm} \leq x \leq 200\,\text{mm}$ (every 20 mm).

Figure 2(c) shows the root mean square (RMS) value of the acoustic pressure around the generated Bessel beam. Figures 3(a)–3(c) show the wind velocity measured with the anemometer around the same beam. It is seen that the measured velocity took its highest value (approximately 3 m/s) around $z = 400\,\text{mm}$ for the upright flow. This demonstrated the mid-air acceleration of an ultrasound-driven flow, which

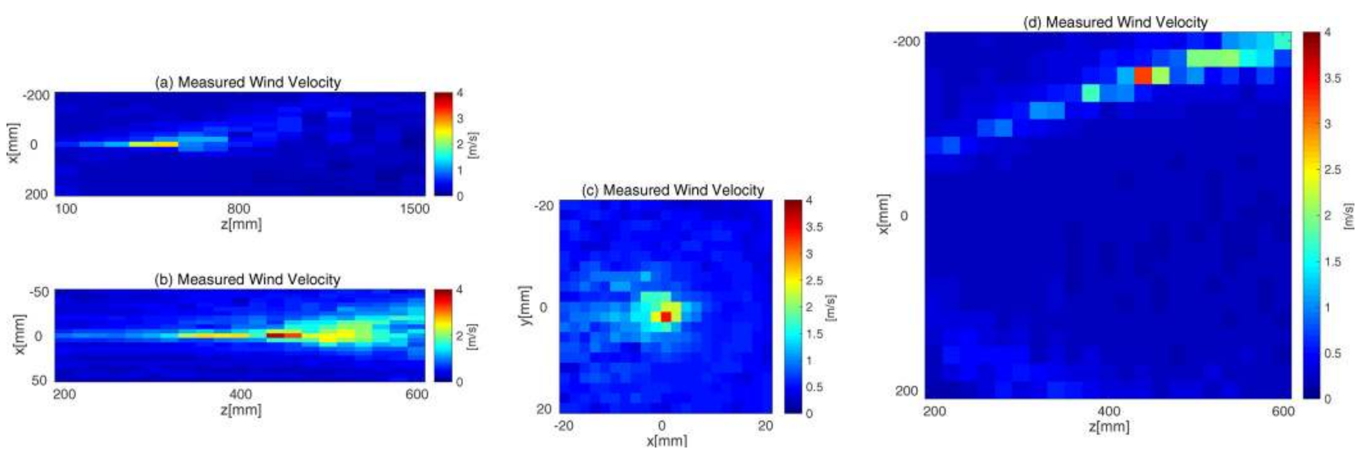

FIG. 3. (a)–(c) Measured spatial distribution of wind velocity in the case of a z-axis parallel beam. These measurements were individually performed with the same upright beam. (d) Measurement results with the same procedure in the case of a tilted beam ($\boldsymbol{v} = [0\ -1\ 0]^T, \theta_{\boldsymbol{v}} = 20°$). $y = 0$ mm for (a), (b), and (d) and $z = 400$ mm for (c).

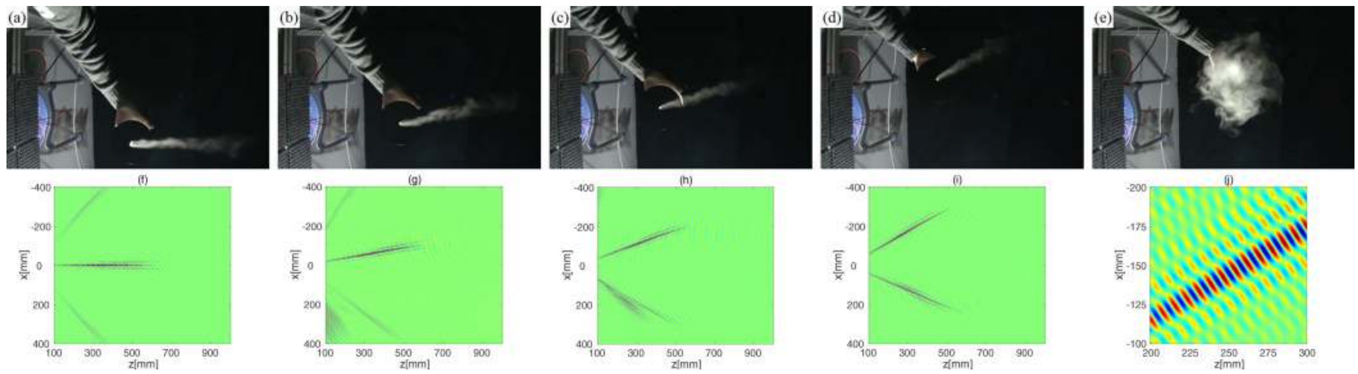

FIG. 4. (a)–(d) Water vapor guided along beam propagation with beam tilt angles of (a) 0°, (b) 10°, (c) 20°, and (d) 30° from left to right. (e) Water vapor spreading without acoustic Bessel beams. (f)–(i) Numerical simulations showing instantaneous signed acoustic pressure distribution corresponding to the cases in (a)–(d), respectively. (j) Magnified graph of (i) indicating the wavefront perpendicular to the beam orientation. We implemented the simulation on MATLAB as a form of the linear pressure superposition from every transducer emission.

is never seen in ordinary jet-driven flows. In addition, spreading of the generated flow seems to have been suppressed within the range of the acoustic beam.

It should be noted that at the depth where the beam is most concentrated (z = 400 mm), most of the velocity of the flow was confined in a circle with a radius of several millimeters.

Figure 3(d) shows that a tilted flow was also generated with the phase shifting technique described above. Figure 4 shows the pictures of water vapor directed in the beam propagation direction and numerical simulations, indicating the pressure of an acoustic Bessel beam with values $\theta_v = 0, 10°, 20°, 30°$ where $\boldsymbol{v} = [0 - 1\ 0]^T$. The simulations indicate that the ghost beams with different propagation directions should also exist. In fact, a careful look at Fig. 3(d) indicates the existence of another weak flow in a different orientation, which looks similar to Fig. 4(h). These "grating lobes" are a common phenomenon created by a set of multiple wave sources. The closer together the sources are arranged the more distant the intervals between each lobe become.

The simulations suggest that the resulting wavefront is perpendicular to the beam orientation. Hence, it is expected that the streaming is driven in the stretching direction of the beam.

Our technique only expresses the flow in the midst of the generated beam, not on the boundary of the beam or outside of it. Since our measurements did not contain "vector" information of the flow field, how particles in the periphery of the beam move remains unclear. While taking the pictures shown in Fig. 4, we noticed that the water vapor was guided in the intended direction only when it was captured at the very center of the beam. A slight deviation from the center would lead the water vapor in a more or less deviated direction (not parallel to the beam propagation direction). In Fig. 4(j), a pair of weaker beams parallel to the primary beam is seen, which is a characteristic energy distribution of Bessel beams. Perhaps, these secondary beams might have caused the changes in the traveling orientation observed when capturing the flow.

As we described above, there was a trade-off between the concentration and the reaching distance of the flow. If one wants a well-concentrated flow over a long distance, using a larger array with more transducers is one solution. This is equivalent to preparing an acoustic lens with a greater aperture. The upper limit for the beam concentration is given by its wavelength, which was 8.5 mm for the phased array used in the experiment. A narrower flow would be possible by using ultrasound transducers with a higher output frequency.

In summary, we reported on the generation of an isolated narrow, straight, long airflow with an ultrasound Bessel beam using an ultrasound phased array. It should be stated that ultrasound phased arrays like the one used in our work have recently become prevalent among those aiming at various applications other than generating acoustic streaming.[25–28] The generated flow based on our technique possesses unique properties, such as detached mid-air blowing points and mid-air acceleration, which may open the door to new applications that are currently inconceivable. For instance, these applications would include the control of mid-air chemical reactions, fine sampling of the spatial distribution of the gas concentration, or even new methods of ethology based on physiological stimulation remotely applied by our technique.

This work was supported by JSPS Kakenhi Grant-in-Aid for Young Scientists (A), 15H05316.

[1]M. Faraday, "On a peculiar class of acoustical figures; and on certain forms assumed by groups of particles upon vibrating elastic surfaces," Philos. Trans. R. Soc. London **121**, 299–318 (1831).
[2]L. Rayleigh, "On the circulation of air observed in Kundt's tube and on some allied acoustic problems," Philos. Trans. R. Soc. London **175-A**, 1–21 (1884).
[3]*Nonlinear Acoustics*, edited by M. F. Hamilton and D. T. Blackstock (Academic Press, San Diego, 1998).
[4]E. N. da C. Andrade, "On the circulation caused by the vibration of air in a tube," Proc. R. Soc. London Ser. A **134**, 445–470 (1931).
[5]W. L. Nyborg, "Acoustic streaming due to attenuated plane wave," J. Acoust. Soc. Am. **25**, 68–75 (1953).
[6]O. V. Rudenko, A. P. Sarvazyan, and S. Y. Emelianov, "Acoustic radiation force and streaming: Induced by focused nonlinear ultrasound in a dissipative medium," J. Acoust. Soc. Am. **99**, 2791–2798 (1996).
[7]S. Nomura, K. Murakami, and Y. Sasaki, "Streaming induced by ultrasonic vibration in a water vessel," Jpn. J. Appl. Phys., Part 1 **39**(6A), 3636–3640 (2000).
[8]A. L. Bernassau, P. G. Jones, F. Gesellchen, M. Riehle, M. Hill, and D. R. S. Cumming, "Controlling acoustic streaming in an ultrasonic heptagonal tweezers with application to cell manipulation," Ultrasonics **54**(1), 268–274 (2014).
[9]J. A. Cosgrove, J. M. Buick, S. D. Pye, and C. A. Greated, "PIV applied to eckart streaming produced by a medical ultrasound transducer," Ultrasonics **39**(6), 461–464 (2001).
[10]L. K. Zarembo, "Acoustic streaming," in *High-Intensity Ultrasonic Fields, Part III*, edited by L. D. Rozenberg (Plenum, 1971), pp. 137–199.

[11]B. Moudjed, V. Botton, D. Henry, H. Ben Hadid, and J.-P. Garandet, "Scaling and dimensional analysis of acoustic streaming jets," Phys. Fluids. **26**, 093602 (2014).
[12]B. Moudjed, V. Botton, D. Henry, S. Millet, J.-P. Garandet, and H. B. Hadid, "Oscillating acoustic streaming jet," Appl. Phys. Lett. **105**, 184102 (2014).
[13]S. J. Lighthill, "Acoustic streaming," J. Sound Vib. **61**, 391–418 (1978).
[14]T. Kamakura, K. Yasuda, and Y. Kumamoto, "Unified description of second-order phenomena in sound waves," Electron. Commun. Jpn. **82**(2), 76–82 (1999).
[15]J. Durnin, J. J. Miceli, Jr., and J. H. Eberly, "Diffraction-free beams," Phys. Rev. Lett. **58**, 1499 (1987).
[16]L. Gong, Y. X. Ren, G. S. Xue, Q. C. Wang, J. H. Zhou, M. C. Zhong, Z. Q. Wang, and Y. M. Li, "Generation of nondiffracting Bessel beam using digital micromirror device," Appl. Opt. **52**(19), 4566–4575 (2013).
[17]W. B. Williams and J. B. Pendry, "Generating Bessel beams by use of localized modes," J. Opt. Soc. Am. A **22**(5), 992–997 (2005).
[18]Y. Monnai, D. Jahn, W. Withayachumnankul, M. Koch, and H. Shinoda, "Terahertz plasmonic Bessel beamformer," Appl. Phys. Lett. **106**(2), 021101 (2015).
[19]P. Lemaitre-Auger, R. Siragusa, C. Caloz, and D. Kaddour, "Circular antenna arrays for near-field focused or multi-focused beams," in *Proceedings of 2013 International Symposium on Electromagnetic Theory* (2013), pp. 425–428.
[20]D. K. Hsu, F. J. Margetan, and D. O. Thompson, "Bessel beam ultrasonic transducer: Fabrication method and experimental results," Appl. Phys. Lett. **55**, 2066–2068 (1989).
[21]P. Katchadjian, C. Desimone, and A. D. Garcia, "Application of Axicon lenses in ultrasonic techniques," AIP Conf. Proc. **1211**, 1043 (2010).
[22]N. Jiménez, V. Romero-García, R. Picó, A. Cebrecos, V. J. Sánchez-Morcillo, L. M. Garcia-Raffi, J. V. Sánchez-Pérez, and K. Staliunas, "Acoustic Bessel-like beam formation by an axisymmetric grating," Europhys. Lett. **106**(2), 24005 (2014).
[23]Y. Li, Z. H. Gu, X. Y. Zou, and J. C. Cheng, "Reflected wavefront manipulation based on ultrathin planar acoustic metasurfaces," Sci. Rep. **3**, 2546 (2013).
[24]L. W. Schmerr, Jr., *Fundamentals of Ultrasonic Phased Arrays* (Springer International Publishing, 2015).
[25]T. Hoshi, M. Takahashi, T. Iwamoto, and H. Shinoda, "Noncontact tactile display based on radiation pressure of airborne ultrasound," IEEE Trans. Haptics **3**, 155–165 (2010).
[26]K. Hasegawa and H. Shinoda, "Aerial display of vibrotactile sensation with high spatial-temporal resolution using large-aperture airborne ultrasound phased array," in *Proceedings of IEEE World Haptics Conference* (2013), pp. 31–36.
[27]M. Fujiwara, K. Nakatsuma, M. Takahashi, and H. Shinoda, "Remote measurement of surface compliance distribution using ultrasound radiation pressure," in *Proceedings of IEEE World Haptics Conference* (2011), pp. 37–43.
[28]A. Marzo, S. A. Seah, B. W. Drinkwater, D. R. Sahoo, B. Long, and S. Subramanian, "Holographic acoustic elements for manipulation of levitated objects," Nat. Commun. **6**, 8661 (2015).